Heliyon 9 (2023) e21059

Contents lists available at ScienceDirect

Heliyon

journal homepage: www.cell.com/heliyon

Plasma exosomal miR-1290 and miR-29c-3p as diagnostic biomarkers for lung cancer

Qian Zhang [a,b,1], Kaifu Zheng [c,1], Yongheng Gao [a,1], Shihong Zhao [a], Yabo Zhao [d], Wangping Li [a], Yandong Nan [a], Zhengping Li [c], Wei Liu [a], Xinxin Wang [a], Yanwei Chen [a,**], Gang Liu [a,***], Faguang Jin [a,*]

[a] Department of Respiratory and Critical Care Medicine, Tangdu Hospital, Air Force Military Medical University, Xi'an, 710038, China
[b] Department of Respiration, Eastern Air Force Hospital, NanJing 210000, China
[c] Department of General Surgery, the 991th Hospital of Joint Logistic Support Force of People's Liberation Army, Xiangyang 441000, China
[d] Department of Thoracic surgery, Tangdu Hospital, Air Force Military Medical University, Xi'an, China

ARTICLE INFO

Keywords:
Diagnosis
Exosome
Lung Neoplasms
MiR-1290
MiR-29c-3p

ABSTRACT

Background: Enhancing the diagnostic efficacy of early-stage lung cancer is crucial for improving prognosis. The objective of this study was to ascertain dependable exosomal miRNAs as biomarkers for the diagnosis of lung cancer.

Methods: Exosomal miRNA candidates were identified through miRNA sequencing and subsequently validated in various case-control sets using real-time quantitative reverse transcription-polymerase chain reaction (RT-qPCR). The correlation between the expression of exosomal miRNAs and the clinicopathological features of lung cancer was investigated. To assess the diagnostic efficacy of exosomal miRNAs for lung cancer, the receiver operating characteristic (ROC) curve analysis was conducted. The optimal cutoff value of exosomal miRNAs was determined in the testing cohort and subsequently confirmed in the validation cohort.

Results: The results showed that the expression of exosomal miR-1290 was significantly elevated, while that of miR-29c-3p was significantly decreased in the plasma of lung cancer patients, especially in those with early-stage lung cancer, compared to individuals with benign lung conditions ($P < 0.01$). Exosomal miR-1290 and miR-29c-3p demonstrated superior diagnostic efficacy compared to conventional tumor biomarkers in distinguishing between lung cancer and benign lung diseases, as evidenced by their respective area under the curve (AUC) values of 0.934 and 0.868. Furthermore, exosomal miR-1290 and miR-29c-3p exhibited higher diagnostic efficiency in early-stage lung cancer than traditional tumor markers, with AUC values of 0.947 and 0.895, respectively. Notably, both exosomal miR-1290 and miR-29c-3p displayed substantial discriminatory capacity in distinguishing between non-small cell lung cancer (NSCLC) and small cell lung cancer (SCLC), as indicated by their respective AUC values of 0.810 and 0.842.

Conclusions: The findings of this study provided evidence that exosomal miR-1290 and miR-29c-3p hold significant potential as biomarkers for the early detection of lung cancer, as well as for differentiating between NSCLC and SCLC.

* Corresponding author.
** Corresponding author
*** Corresponding author
E-mail addresses: chenyw@szu.edu.cn (Y. Chen), gangliu_guangyi@163.com (G. Liu), jinfag@fmmu.edu.cn (F. Jin).
[1] These authors have contributed equally to this work.

https://doi.org/10.1016/j.heliyon.2023.e21059
Received 21 July 2023; Received in revised form 7 October 2023; Accepted 13 October 2023
Available online 17 October 2023

1. Introduction

Lung cancer ranks as the second most prevalent form of cancer globally and is the primary cause of cancer-related mortality. It constitutes 11.4 % of newly diagnosed cancer cases and accounts for 18 % of cancer-related deaths [1]. Non-small cell lung cancer (NSCLC) represents the predominant histopathological subtype of lung cancer, encompassing 85 % of all primary lung cancer instances [2]. The five-year survival rate for NSCLC is contingent upon the clinical stage, exhibiting significant variation from 57 % for patients diagnosed with stage I NSCLC to a mere 4 % for those with stage IV NSCLC. Nevertheless, the majority of patients (61 %) receive a diagnosis of advanced NSCLC at the time of detection [3]. Hence, it is imperative to enhance the diagnostic efficacy of early-stage lung cancer in order to enhance the prognosis.

Low-dose computed tomography (LDCT) is the endorsed screening modality that diminishes lung cancer mortality by 20 %. Nevertheless, the elevated rate of false-positive results associated with LDCT may lead to excessive diagnosis and unwarranted treatment. Additionally, the repetitive nature of scanning incurs financial burdens and exposes individuals to radiation [4,5]. The diagnostic utility of conventional serum tumor markers, such as carcinoembryonic antigen (CEA), ferritin (FRT), neuron-specific enolase (NSE), carbohydrate antigen 125 (CA125), cytokeratin 19 fragment 21-1 (CYFRA21-1), squamous cell carcinoma antigen (SCC), and carbohydrate antigen 50 (CA50), is constrained by their inadequate sensitivity and specificity, particularly in the context of early-stage lung cancer detection [6]. Pathological biopsy, being the established benchmark for diagnosing lung cancer, is an invasive detection technique that augments the likelihood of tumor dissemination and exhibits inadequate repeatability. Additionally, the biopsy tissue solely provides insight into the localized tumor condition and transient patient information, disregarding the fact that cancer progression is a dynamic and heterogeneous phenomenon [7–9].

Liquid biopsy is a burgeoning detection technique that relies on the identification of tumor constituents in bodily fluids. This method effectively addresses the constraints associated with tissue biopsy by virtue of its non-invasive nature, commendable reproducibility, and capacity to furnish more precise insights into the systemic burden of tumors. Exosomes, extensively explored in diverse pathological conditions, are abundantly present in various bodily fluids, rendering them readily detectable in liquid biopsies [10,11]. Cancer-derived miRNAs can be selectively enriched and encapsulated in exosomes, which are more stable due to the presence of a lipid bilayer membrane [12]. An increasing number of studies have revealed that exosomal miRNAs play a crucial role in the initiation and progression of lung cancer, primarily through mechanisms such as angiogenesis, epithelial mesenchymal transformation, drug resistance, and immune evasion [13]. Consequently, exosomal miRNAs hold promise as potential diagnostic and prognostic biomarkers for lung cancer. However, it is important to note that the diagnostic efficiency of most exosomal miRNAs remains limited, particularly in the context of early-stage lung cancer. Hence, the pursuit of exosomal miRNAs exhibiting enhanced diagnostic efficacy and improved stability holds immense importance in the realm of lung cancer diagnosis and treatment.

The objective of this study was to ascertain dependable plasma exosomal miRNAs as biomarkers for the identification of lung cancer. Through the utilization of miRNA-seq, exosomal miRNA profiling was conducted between the lung cancer and control groups, leading to the identification of potential exosomal miRNA candidates. These candidates were subsequently validated across multiple case-control cohorts. Furthermore, the diagnostic potential of exosomal miRNAs was assessed by employing a receiver operating characteristic (ROC) curve.

2. Materials and methods

2.1. Study subjects and sample collection

All participants in this study were enrolled at the Second Affiliated Hospital of Air Force Military Medical University from November 2020 to August 2021. Prior to sample collection, none of lung cancer patients included in this study had received any form of antitumor treatment. The control group comprised individuals with benign pulmonary disease and no previous history of cancer. Detailed clinical and histopathological data, such as age, sex, smoking history, clinical stage, pathological type, and differentiation grade, were meticulously documented. Early-stage lung cancer was defined as stage I-II of lung cancer. This study was approved by the Medical Ethics Committee of the Second Affiliated Hospital of Air Force Military Medical University (K202011-14) and written informed consent was obtained from each participant.

2.2. Study design

A multi-stage case-control study was undertaken to ascertain the potential of plasma exosomal miRNAs as non-invasive biomarkers for lung cancer. The study encompassed four distinct stages, namely screening, training, testing, and validation (Fig. 1). During the screening phase, exosomal miRNA profiling was conducted via small RNA sequencing in a cohort comprising four lung cancer cases and four controls. Subsequently, four promising exosomal miRNAs were selected and subjected to preliminary assessment in a training cohort comprising 12 lung cancer patients and seven controls. The expression levels of hsa-miR-1290 and hsa-miR-29c-3p, among the four exosomal miRNAs, exhibited significant differences between the lung cancer and control groups. Subsequently, these two miRNAs were subjected to further evaluation in both the testing cohort (consisting of 41 lung cancer patients and 19 control individuals) and the validation cohort (comprising 38 lung cancer patients and 19 control individuals) using the real-time quantitative reverse transcription-polymerase chain reaction (RT-qPCR) technique. In both subsequent stages, the two exosomal miRNAs continued to demonstrate significant differences between the lung cancer and control groups. The two miRNAs were subsequently assessed in tissue

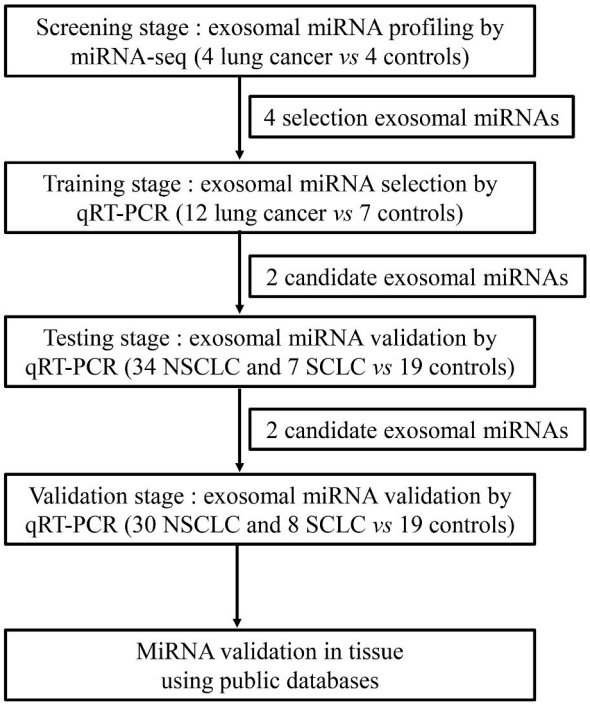

Fig. 1. Flow chart showing the study design.

specimens through the utilization of the Gene Expression Omnibus (GEO) database.

2.3. Isolation and identification of plasma exosomes

Peripheral venous blood was collected from each participant in a tube containing ethylenediaminetetraacetic acid (EDTA). Plasma was isolated using a two-step centrifugation regimen (1200×*g* for 10 min at 4 °C followed by 1800×*g* for 10 min at 4 °C) within 1 h and immediately stored in RNase-free tubes at −80 °C until exosome isolation. A volume of 1.5 ml of subject plasma was diluted in phosphate buffered saline (PBS) to a final volume of 10 ml. The sample was then subjected to differential centrifugation at 500×*g* for 5 min at 4 °C, 2000×*g* for 30 min at 4 °C, followed by 10000×*g* for 45 min at 4 °C. Subsequently, the supernatant underwent filtration using a 0.45 μm membrane filter and was subjected to ultracentrifugation at 100 000×*g* for 70 min at 4 °C. The resulting pellet was resuspended in PBS and subjected to a second round of ultracentrifugation at 100 000×*g* for 70 min at 4 °C. The obtained exosomes were then resuspended in PBS and stored at −80 °C. To ascertain the presence of exosomes, techniques such as transmission electron microscopy (TEM), nanoparticle characterization, and western blotting were employed.

2.4. Exosomal miRNA profiling using small RNA sequencing

MicroRNAs were extracted from plasma-derived exosomes utilizing TRIzol LS Reagent (Invitrogen, Carlsbad, California, USA). The QC results of purified RNA were showed in Table S1. Subsequently, microRNA sequence analysis was conducted employing the Illumina NextSeq 500 platform (Illumina, San Diego, California, USA). The steps involved in library preparation for miRNA-seq and the reads generated by each sample were showed in Table S2 and Table S3. The raw data underwent filtration to eliminate unqualified reads, resulting in the acquisition of clean data. These clean data were then aligned against the miRNA sequence from miRbase (Release 22) using Bowtie [14]. Normalization of miRNA expression was achieved by calculating the number of reads per million (RPM). Differentially expressed exosomal miRNAs between groups were identified using edgeR [15,16] with the default threshold of $|\log2 \text{(fold change)}| \geq 1.5$ and *P*-value <0.05.

2.5. Exosomal miRNA quantification using RT-qPCR

The miRNA was subjected to reverse transcription (RT) to generate complementary DNA (cDNA) using a stem-loop RT method. This process involved incubation at 16 °C for 30 min, 42 °C for 40 min, and 85 °C for 5 min. The specific RT primers for miRNA were employed, and their details can be found in Table S4. For real-time quantitative polymerase chain reaction (qPCR), the PCR Master Mix (Aksomics, Shanghai, China), miRNA-specific primer, and cDNA template were combined in reaction mixtures. These mixtures were then subjected to incubation at 95 °C for 10 min, followed by 40 cycles of amplification at 95 °C for 15 s and 60 °C for 1 min using a

QuantStudio 5 real-time PCR System (Applied Biosystems, New York, USA). As previously mentioned, the $2^{-\Delta\Delta CT}$ method was employed to calculate the relative expression levels of the miRNAs [17]. Hsa-miR-423-5p was utilized as a reference for normalizing the expression of the target miRNA through RT-qPCR. The primer sequences employed in qPCR can be found in Table S5.

2.6. Bioinformatics analysis

The targets of exosomal miRNAs were determined using TargetScan and miRDB databases, and the overlapping targets from both databases were selected for further analysis. Gene ontology (GO) enrichment analysis was conducted to ascertain the molecular function, cellular composition, and biological processes associated with the target genes, and the Kyoto Encyclopedia of Genes and Genomes (KEGG) pathway analysis was employed to ascertain the biological pathways associated with the target genes.

2.7. Statistic analysis

The determination of the sample size was conducted by employing an online sample calculator available at http://powerandsamplesize.com/. The calculation of the sample size was performed with a power of 80 %, a significance level of 0.05, and a two-sided test. Categorical variables were assessed using either the chi-square test or Fisher's exact test, while quantitative data were analyzed using the *t*-test or Mann-Whitney *U* test. The diagnostic efficacy of exosomal miRNAs was evaluated through ROC analysis, which included the calculation of the area under the curve (AUC), sensitivity, and specificity. Med-Calc 18.2.1 (Med-Calc software, Ostend, Belgium) was utilized for this analysis. The optimal cutoff value for exosomal miRNAs was determined using the Youden index. Statistical significance was defined as a two-tailed *P*-value <0.05. SPSS 22.0 (IBM, Armonk, NY, USA) and GraphPad Prism 8.0 (GraphPad Software, CA, USA) were used for data analysis and graphing.

3. Results

3.1. Clinicopathological characteristics of participants

The clinicopathological characteristics of the testing group (consisting of 41 lung cancer cases and 19 controls) and the validation group (comprising 38 lung cancer cases and 19 controls) are presented in Table 1. Within the testing group, there were 11 patients diagnosed with stage I–II lung cancer and 30 patients diagnosed with stage III–IV lung cancer. Similarly, the validation group included 10 patients with stage I–II lung cancer and 28 patients with stage III–IV lung cancer. Furthermore, the testing group consisted of 34 patients with NSCLC and 7 patients with small cell lung cancer (SCLC), while the validation group consisted of 30 patients with NSCLC and 8 patients with SCLC.

Table 1
Clinicopathological characteristics of lung cancer patients and control populations.

Characteristics	Testing group			Validation group		
	Lung cancer (n = 41)	Control (n = 19)	P-value	Lung cancer (n = 38)	Control (n = 19)	P-value
Age, n (%)			0.552			0.244
≤ 60 years	14 (34.1)	8 (42.1)		12 (31.6)	9 (47.4)	
> 60 years	27 (65.9)	11 (57.9)		26 (68.4)	10 (52.6)	
Sex, n (%)			0.631			0.730
Male	32 (78.0)	13 (68.4)		29 (76.3)	16 (84.2)	
Female	9 (22.0)	6 (31.6)		9 (23.7)	3 (15.8)	
Smoking Index			0.083			0.178
< 400	14 (34.1)	11 (57.9)		21 (55.3)	14 (73.7)	
≥ 400	27 (65.9)	8 (42.1)		17 (44.7)	5 (26.3)	
TNM stage			/			/
I-II	11 (26.8)	/		10 (26.3)	/	
III-IV	30 (78.9)	/		28 (73.7)	/	
Pathological type			/			/
NSCLC	34 (82.9)	/		30 (78.9)	/	
LUAD	19 (46.3)	/		16 (42.1)	/	
LUSC	15 (36.6)	/		14 (36.8)	/	
SCLC	7 (17.1)	/		8 (21.1)	/	
Differentiation grade for NSCLC			/			/
Poor	11 (32.4)	/		12 (40.0)	/	
Moderate	3 (8.8)	/		4 (13.3)	/	
Well	10 (29.4)	/		6 (20.0)	/	
Unknown	10 (29.4)	/		8 (26.7)	/	

LUAD, lung adenocarcinoma; LUSC, lung squamous cell carcinoma; NSCLC, non-small cell lung cancer; SCLC, small cell lung cancer; TNM, tumor-node-metastasis.

3.2. Identification of exosomes

The TEM images demonstrated that the isolated vesicles exhibited a characteristic bilayer morphology and displayed the anticipated size distribution of exosomes, as depicted in Fig. 2A. Furthermore, nanoflow analysis indicated that the vesicles obtained from plasma had an average diameter of approximately 72 nm, as illustrated in Fig. 2B. Moreover, the presence of exosome-positive markers (CD63 and TSG101) was detected in the isolated vesicles, while their absence was observed in the exosome-depleted supernatant (Fig. 2C, Fig. S1 and Fig. S2). Conversely, the negative marker GM130 was underrepresen tation in the isolated vesicles (Fig. 2C and Fig. S3). These findings provide compelling evidence for the successful isolation of exosomes from plasma.

3.3. Selection of candidate exosomal miRNAs

Exosomal microRNA sequencing was conducted on a cohort consisting of four lung cancer patients and four control subjects, with the aim of identifying a panel of exosomal miRNAs that could potentially serve as biomarkers for lung cancer. A comprehensive analysis was conducted on a total of 890 detectable exosomal miRNAs to ascertain the differential expression of miRNAs between the two groups. The findings revealed a total of five significantly upregulated miRNAs and 52 significantly downregulated miRNAs, as depicted in Fig. 3, Fig. S4 and Excel S1. Among the miRNAs that exhibited a $|\log2(\text{fold change})| \geq 3$, taking into account the RPM of each sample and the biological functions of miRNAs, we identified one upregulated miRNA (miR-1290) and three downregulated miRNAs (miR-29c-3p, miR-129-5p, and miR-145-5p) as potential exosomal miRNA candidates.

3.4. Evaluation of candidate exosomal miRNAs using RT-qPCR

These candidate exosomal miRNAs were initially assessed in the training cohort. As depicted in Fig. 4A–D, exosomal miR-1290 displayed a significant upregulation, while miR-29c-3p exhibited a significant downregulation in the lung cancer group compared

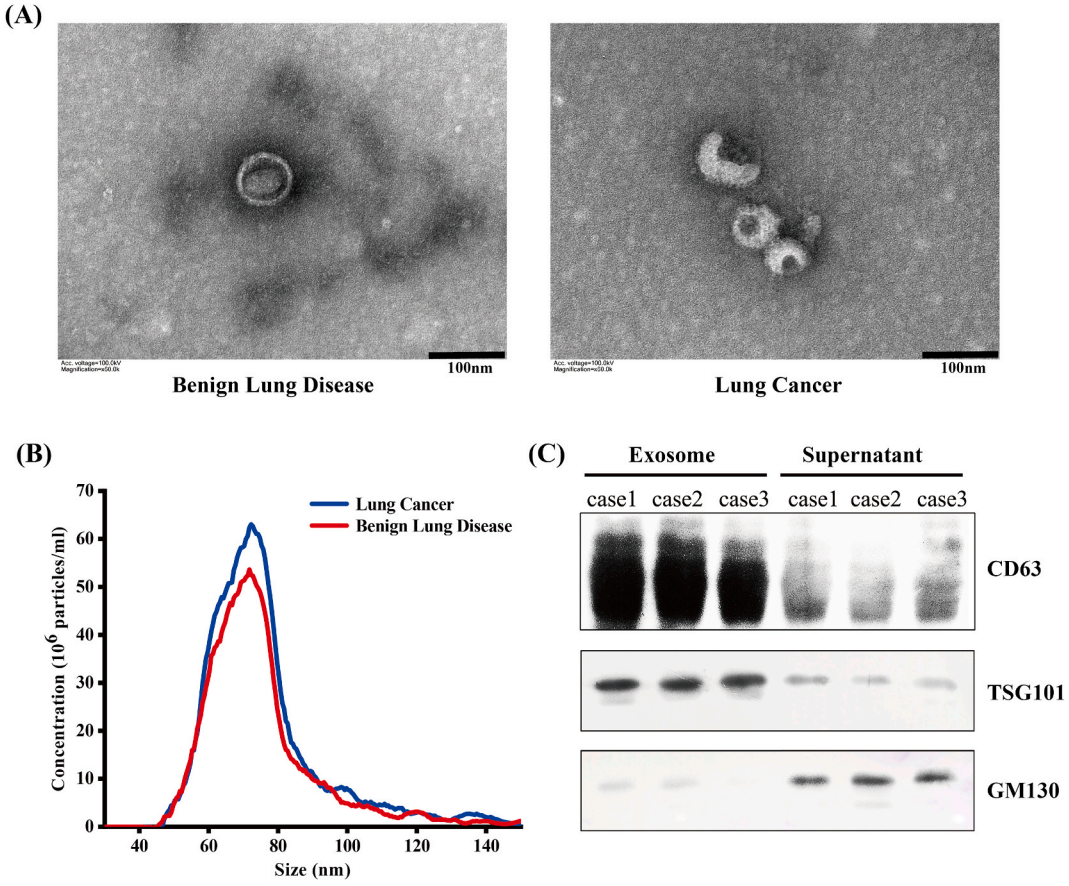

Fig. 2. Identification of exosomes derived from plasma. (A) transmission electron microscopy (TEM) images revealed the typical morphology and size of exosomes. Scale bar, 100 nm **(B)** nano flow analysis of the size distribution and concentration of exosomes **(C)** Western blot for specific exosome markers CD63, TSG101, and GM130 in plasma exosomes and exosome-depleted supernatant.. (The grouping of blots of each marker was obtained from the same gel. And full-length gels and blots can be seen in additional files.)

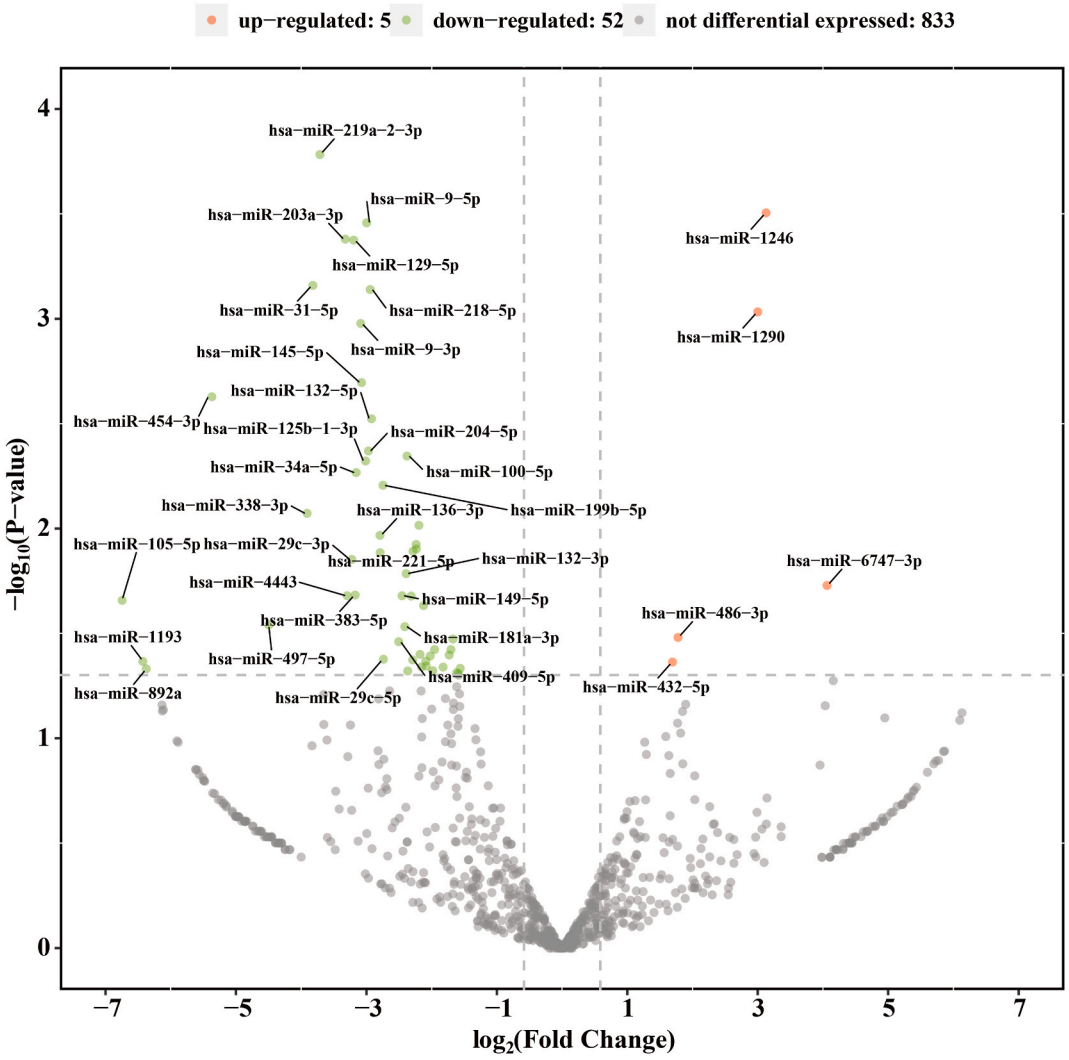

Fig. 3. Volcano Plot showing the differential expression of exosomal miRNAs between lung cancer and benign lung disease.

to the control group ($P < 0.01$). The expression of miR-145-5p exhibited an increase in the lung cancer group as compared to the control group, which contradicted its expression pattern observed during the screening stage. Furthermore, there were no significant differences in the levels of exosomal miR-129-5p between the lung cancer and control groups. Consequently, exosomal miR-1290 and miR-29c-3p were chosen for subsequent experiments.

During the testing stage, exosomal miR-1290 demonstrated a significant upregulation, while miR-29c-3p exhibited a significant downregulation in lung cancer patients compared to controls ($P < 0.001$) (Fig. 4E and F). Significantly increased levels of exosomal miR-1290 and significantly decreased levels of miR-29c-3p were observed in samples from patients diagnosed with early lung cancer compared to controls ($P < 0.01$) (Fig. 4G and H). The expression patterns of exosomal miR-1290 and miR-29c-3p in the validation cohort were consistent with the findings from the testing stage, indicating their potential as biomarkers for all lung cancer patients and early lung cancer cases ($P < 0.001$) (Fig. 4I-L).

3.5. Correlations between exosomal miRNAs and clinicopathological characteristics of lung cancer

The correlations between the expression levels of exosomal miRNAs and clinicopathological features of lung cancer patients were further evaluated. The results presented in Table 2 indicated a significant upregulation of exosomal miR-1290 in patients with advanced lung cancer compared to those with early-stage lung cancer ($P < 0.01$). Additionally, the expression level of miR-1290 was significantly higher in patients with distant metastasis compared to those without distant metastasis ($P < 0.05$). Moreover, the expression of miR-1290 was found to be significantly elevated in the NSCLC group compared to the SCLC group, whereas the expression of miR-29c-3p was notably lower in the NSCLC group compared to the SCLC group ($P < 0.001$).

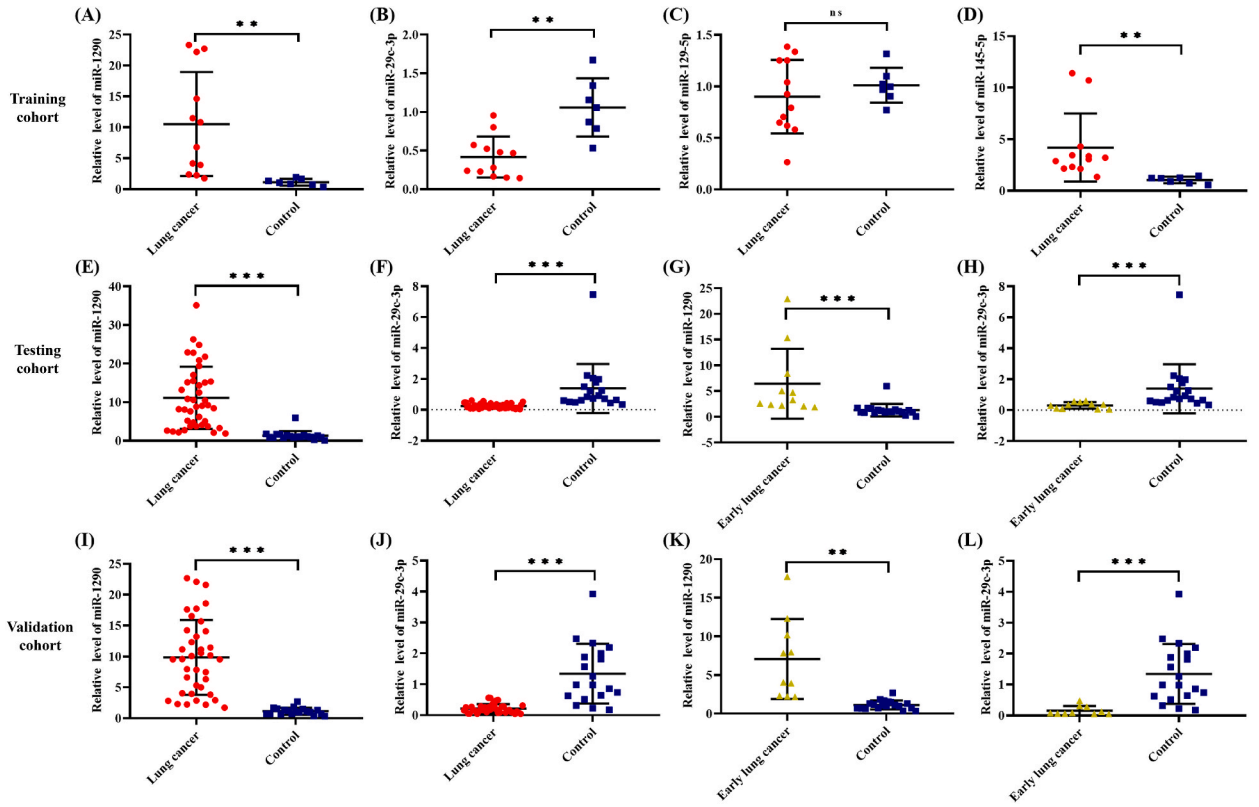

Fig. 4. Differential expression of exosomal miRNAs between patients with lung cancer/early lung cancer and controls. The expression levels of miR-1290 **(A)**, miR-29c-3p **(B)**, miR-129-5p **(C)**, and miR-145-5p **(D)** in the training cohort. The expression levels of miR-1290 and miR-29c-3p in the testing cohort between all lung cancer samples and controls **(E, F)**, and between early lung cancer samples and controls **(G, H)**. The expression levels of miR-1290 and miR-29c-3p in the validation cohort between all lung cancer samples and controls **(I, J)**, and between early lung cancer samples and controls **(K, L)**. ***, $P < 0.001$; **, $P < 0.01$.

3.6. The diagnostic efficacy and cutoff value of exosomal miRNAs in the testing cohort

In order to assess the diagnostic effectiveness of exosomal miRNAs in lung cancer, ROC curves were constructed to determine the AUC, sensitivity, specificity, and optimal cutoff values during the testing phase. Exosomal miR-1290 and miR-29c-3p exhibited a high diagnostic capacity in distinguishing lung cancer from benign diseases, with AUC values of 0.982 (95 % confidence interval [CI]: 0.908–0.999) and 0.970 (95 % CI: 0.890–0.997), respectively. Based on the analysis of the ROC curve, it was determined that the optimal cutoff value for miR-1290 was 1.747, resulting in a sensitivity of 100 % and a specificity of 94.74 %. Similarly, the optimal cutoff value for miR-29c-3p was found to be 0.426, with corresponding sensitivity and specificity values of 87.8 % and 94.74 %, respectively (Fig. 5A and B). Furthermore, the exosomal miR-1290 and miR-29c-3p also exhibited a significant discriminatory capacity in distinguishing early-stage lung cancer from benign diseases. The AUC for miR-1290 was calculated to be 0.962 (95 % CI: 0.820–0.999), with a sensitivity of 100 % and a specificity of 94.74 % at the cutoff value of 1.747. The AUC for miR-29c-3p was determined to be 0.923 (95 % CI: 0.766–0.988), with a sensitivity of 100 % and specificity of 73.68 % at a cutoff value of 0.602 (Fig. 5C and D).

3.7. Diagnostic efficacy of exosomal miRNAs in the validation cohort

To verify the diagnostic efficiency of miR-1290 and miR-29c-3p furtherly and for the clinic convenience, all patients in the validation cohort were further divided into a “miRNA positive group” and a “miRNA negatived group” based on the cutoff value formulated in the testing stage. Then ROC curve was used to evaluate the sensitivity and specificity of exosomal miRNAs. According to the data presented in Table 3, both exosomal miR-1290 and miR-29c-3p exhibited significantly greater discriminatory ability between lung cancer and benign lung diseases when compared to traditional tumor markers (CEA, FRT, NSE, CA125, CYFRA211, SCC, and CA50). Exosomal miR-1290 demonstrated a high diagnostic capacity in discriminating lung cancer from controls, as evidenced by an AUC of 0.934 (95 % CI: 0.836–0.983), a sensitivity of 97.37 %, and a specificity of 89.47 %. Similarly, exosomal miR-29c-3p displayed an AUC of 0.868 (95 % CI: 0.753–0.943) to discriminate lung cancer from controls, along with a sensitivity of 89.47 % and a specificity of 84.21 % (Fig. 5E and F). Furthermore, the diagnostic efficacy of exosomal miR-1290 and miR-29c-3p in distinguishing early-stage

Table 2
Correlation between the expression levels of exosomal miRNA and clinicopathological characteristics.

Characteristics	Number	miR-1290	P-value	miR-29c-3p	P-value
Age			0.323		0.247
≤60 years	26	8.02 (3.51–14.45)		0.26 (0.12–0.34)	
> 60 years	53	9.57 (5.11–16.03)		0.16 (0.10–0.29)	
Sex			0.752		0.132
Male	61	9.07 (4.00–15.12)		0.20 (0.11–0.33)	
Female	18	10.32 (4.03–15.94)		0.15 (0.08–0.26)	
Smoking Index			0.745		0.418
< 400	35	9.53 (5.02–15.34)		0.19 (0.09–0.28)	
≥ 400	44	9.32 (3.76–15.14)		0.17 (0.11–0.35)	
Clinical stage			<0.01		0.491
I-II	21	4.06 (2.28–9.30)		0.12 (0.06–0.37)	
III-IV	58	10.56 (6.29–15.91)		0.19 (0.13–0.29)	
T stage			<0.05		0.382
T1-T2	37	7.84 (2.72–14.16)		0.16 (0.08–0.32)	
T3-T4	42	10.27 (6.29–15.78)		0.19 (0.13–0.32)	
Lymphatic metastasis			0.107		0.543
Negative	19	9.22 (4.06–11.16)		0.12 (0.08–0.38)	
Positive	60	9.53 (3.99–16.32)		0.19 (0.12–0.30)	
Distant metastasis			<0.01		0.514
Negative	31	5.05 (2.37–14.09)		0.16 (0.08–0.34)	
Positive	48	10.51 (6.61–16.19)		0.19 (0.11–0.31)	
Pathological type			<0.001[a]		<0.001[a]
NSCLC	64	10.71 (6.61–16.32)		0.16 (0.09–0.28)	
LUAD	35	10.08 (4.06–17.62)	0.848[b]	0.14 (0.09–0.28)	0.454[b]
LUSC	29	11.16 (8.07–15.61)		0.16 (0.11–0.28)	
SCLC	15	3.82 (2.92–5.33)		0.41 (0.26–0.47)	
Differentiation grade for NSCLC			0.215		0.893
Poor	23	10.19 (5.05–14.23)		0.16 (0.09–0.31)	
Moderate	7	4.06 (2.31–22.91)		0.14 (0.08–0.29)	
Well	16	11.80 (9.00–17.87)		0.16 (0.13–0.21)	
Unknown	18	/		/	

LUAD, lung adenocarcinoma; LUSC, lung squamous cell carcinoma; NSCLC, non-small cell lung cancer; SCLC, small cell lung cancer; TNM, tumor-node-metastasis; [a] NSCLC vs SCLC; [b] LUAD vs LUSC.

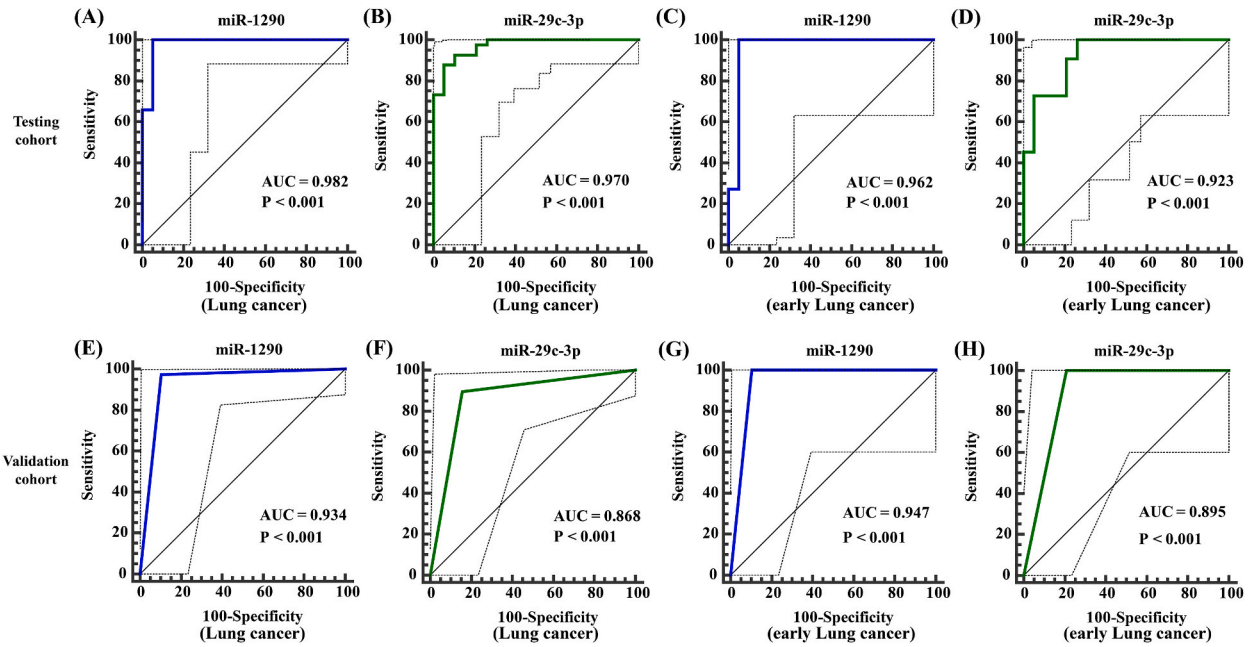

Fig. 5. ROC curves of exosomal miR-1290 and miR-29c-3p for diagnosis of lung cancer. ROC curves of miR-1290 and miR-29c-3p to distinguish lung cancer from benign lung disease **(A, B)**, and to distinguish early lung cancer from benign lung disease **(C, D)** in the testing cohort. ROC curves of miR-1290 and miR-29c-3p to distinguish lung cancer from benign lung disease **(E, F)**, and to distinguish early lung cancer from benign lung disease **(G, H)** in the validation cohort. ROC, receiver operating characteristic; AUC, area under the curve.

Table 3
The diagnostic efficacy of exosomal miRNAs for lung cancer in the validation cohort.

Exosomal miRNAs	AUC (95 % CI)	Sensitivity (%)	Specificity (%)	P-value
miR-1290	0.934 (0.836–0.983)	97.37	89.47	<0.001
miR-29c-3p	0.868 (0.753–0.943)	89.47	84.21	<0.001
CEA	0.737 (0.603–0.845)	57.89	89.47	<0.001
FRT	0.618 (0.480–0.744)	28.95	94.74	<0.01
NSE	0.737 (0.603–0.845)	63.16	84.21	<0.001
CA125	0.711 (0.575–0.823)	47.37	94.74	<0.001
CYFRA211	0.724 (0.589–0.834)	55.26	89.47	<0.001
SCC	0.539 (0.402–0.672)	7.89	100.00	0.075
CA50	0.605 (0.467–0.732)	21.05	100.00	<0.01

AUC, area under the curve; CI, confidence interval; CEA, carcinoembryonic antigen; CA125, carbohydrate antigen 125; CYFRA21-1, cytokeratin 19 fragment 21-1; CA50, carbohydrate antigen 50; FRT, ferritin; NSE, neuron specific enolase; SCC, squamous cell carcinoma antigen.

lung cancer from benign lung diseases was found to be significantly superior to that of conventional tumor markers. The AUC for miR-1290 was determined to be 0.947 (95 % CI: 0.795–0.996), with a sensitivity of 100 % and specificity of 89.47 %. Similarly, the AUC for miR-29c-3p was calculated to be 0.895 (95 % CI: 0.724–0.977), with a sensitivity and specificity of 100 % and 78.95 %, respectively (Table 4, Fig. 5G and H).

3.8. Discriminatory capability of exosomal miRNAs for lung cancer with different pathological subtype and clinical stage

The discriminatory potential of exosomal miRNAs was assessed according to the associations between exosomal miRNAs and clinicopathological characteristics of patients with lung cancer. The testing cohort and validation cohort were combined, resulting in a total of 64 patients with NSCLC and 15 patients with SCLC included in the analysis. Subsequently, the discriminatory capability of exosomal miR-1290, miR-29c-3p, and the combination of miR-1290 and miR-29c-3p were separately analyzed. The findings revealed that both exosomal miR-1290 and miR-29c-3p demonstrated a high discriminatory ability between NSCLC and SCLC, with an AUC of 0.810 (95 % CI: 0.707–0.890) and 0.842 (95 % CI: 0.742–0.914), respectively (Fig. 6A and B). Moreover, the combination of miR-1290 and miR-29c-3p exhibited superior diagnostic efficiency compared to individual miRNAs (Fig. 6C). Further, exosomal miR-1290 exhibited a significant ability in differentiating early lung cancer patients from advanced lung cancer patients (AUC: 0.743, 95 % CI: 0.632–0.835) and distinguish lung cancer patients with distant metastasis from those without distant metastasis (AUC: 0.681, 95 % CI: 0.567–0.782), as indicated in Table S6.

3.9. Expression and prognostic value of miRNAs in lung cancer tissues

The expression levels of miR-1290 and miR-29c-3p were further examined in lung cancer and normal lung tissues using data from the GEO database. The specific datasets analyzed in this study were presented in Table S7. In accordance with the expression trend observed in plasma exosomes, the expression of miR-29c was significantly downregulated in lung cancer tissues compared to normal lung tissues, as evidenced by the data from GSE48414, GSE63805, GSE19945, GSE102286, GSE53882, and GSE15008 (Fig. 7A–C, Figs. S5A–C). Conversely, the levels of miR-1290 in lung cancer tissues were found to be significantly higher than those in normal lung tissues, as indicated by the data from GSE48414, GSE63805, GSE19945, and GSE102286 (Fig. 7D–F, Fig. S5D). And the expression of miR-1290 did not exhibit significant differences in GSE53882 and was not detected in GSE15008 (Fig. S5E). The prognostic significance of miRNAs in lung cancer was assessed using data from The Cancer Genome Atlas (TCGA) database. Analysis of Kaplan-Meier curves revealed that lower levels of miR-29c expression in lung adenocarcinoma patients may be associated with a poorer prognosis ($P = 0.059$) (Fig. 7G). Additionally, lung adenocarcinoma patients with high miR-1290 expression had a significantly shorter overall survival time compared to those with low miR-1290 expression ($P < 0.05$) (Fig. 7H). However, the expression of both miR-29c and miR-1290 did not show any correlation with the survival of patients with lung squamous cell carcinoma in TCGA (Fig. S6).

Table 4
The diagnostic efficacy of exosomal miRNAs for early-stage lung cancer in the validation cohort.

Exosomal miRNAs	AUC (95 % CI)	Sensitivity (%)	Specificity (%)	P-value
miR-1290	0.947 (0.795–0.996)	100.00	89.47	<0.001
miR-29c-3p	0.895 (0.724–0.977)	100.00	78.95	<0.001
CEA	0.597 (0.400–0.774)	30.00	89.47	0.249
FRT	0.574 (0.377–0.754)	20.00	94.74	0.304
NSE	0.621 (0.423–0.793)	40.00	84.21	0.190
CA125	0.526 (0.334–0.713)	100.00	5.26	0.317
CYFRA211	0.547 (0.353–0.732)	20.00	89.47	0.532
SCC	0.500 (0.310–0.690)	0.00	100.00	1.000
CA50	0.550 (0.355–0.734)	10.00	100.00	0.317

AUC, area under the curve; CI, confidence interval; CEA, carcinoembryonic antigen; CA125, carbohydrate antigen 125; CYFRA21-1, cytokeratin 19 fragment 21-1; CA50, carbohydrate antigen 50; FRT, ferritin; NSE, neuron specific enolase; SCC, squamous cell carcinoma antigen.

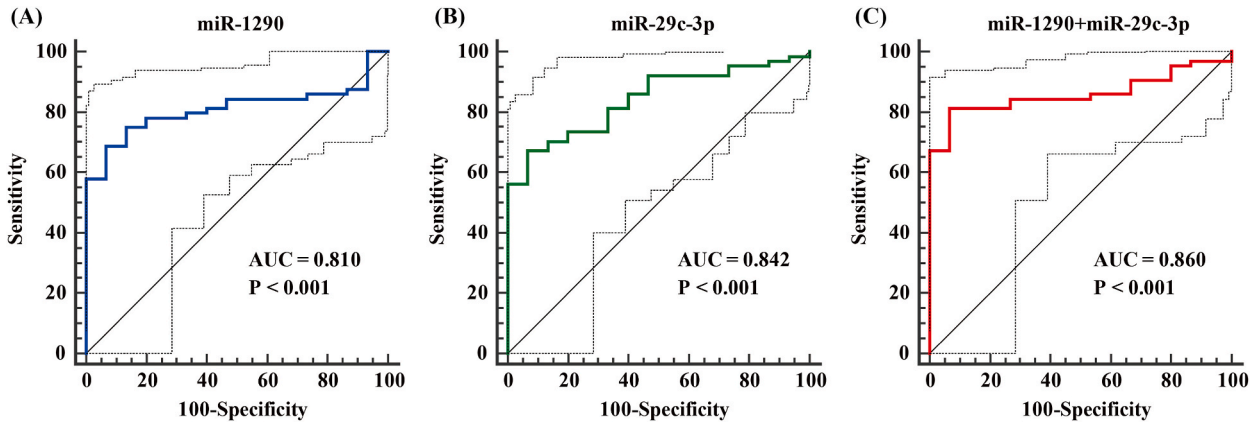

Fig. 6. ROC curves of exosomal miR-1290 and miR-29c-3p to distinguish NSCLC from SCLC. ROC curve of miR-1290 or miR-29c-3p to distinguish NSCLC from SCLC **(A, B)**. ROC curve of a combination of miR-1290 and miR-29c-3p to distinguish NSCLC from SCLC (**C**). ROC, receiver operating characteristic; AUC, area under the curve; NSCLC, non-small cell lung cancer; SCLC, small cell lung cancer.

3.10. Bioinformatics analysis of candidate exosomal miRNAs

The identification of target genes for exosomal miR-1290 and miR-29c-3p was accomplished through a comprehensive analysis of the miRDB and TargetScan databases (Excel S2 and Excel S3). A total of 90 potential target genes for miR-1290 and 279 potential target genes for miR-29c-3p were successfully identified (Fig. S7). The results of GO analysis revealed that miR-1290 exhibited a strong correlation with the regulation of protein kinase A signaling, cell junction components, and the extracellular matrix (Fig. 8). On the other hand, miR-29c-3p was found to be associated with the extracellular matrix, collagen binding, and platelet-derived growth factor binding (Fig. 9). KEGG analyses demonstrated the involvement of miR-1290 in multiple cancer-related pathways, namely tight junction, glycolysis/gluconeogenesis, and fatty acid metabolism. And miR-29c-3p was found to be implicated in other tumor-associated pathways, including the PI3K-Akt signaling pathway, pathways in cancer, and SCLC (Fig. 10A and B).

4. Discussion

Despite notable advancements in the diagnosis and treatment of lung cancer in recent decades, the prognosis of this disease remains unfavorable primarily due to challenges associated with early detection [3,18]. Exosomal miRNAs derived from tumors exhibit notable stability, selective enrichment properties, and disease-specific characteristics [12,19], playing a crucial role in the oncogenesis and progression of lung cancer. Considerable attention has been directed towards exosomal miRNAs as potential biomarkers for the diagnosis and prognosis of lung cancer [13]. In this investigation, a comprehensive analysis of exosomal miRNA profiling was conducted using miRNA-seq, leading to the identification of four specific exosomal miRNAs (miR-1290, miR-29c-3p, miR-129-5p, and miR-145-5p) that were subsequently chosen for further validation. In comparison to benign lung disease, the expression of exosomal miR-1290 was notably increased while miR-29c-3p was significantly decreased in lung cancer. Likewise, lung cancer tissue samples exhibited higher levels of miR-1290 and lower levels of miR-29c-3p compared to normal tissue samples. These findings provided evidence that the aberrant expression of exosomal miR-1290 and miR-29c-3p was derived from the tumor.

Previous research has also documented elevated expression of exosomal miR-1290 in various cancer types [20–23]. MiR-1290 has been observed to frequently function as an onco-miRNA in lung cancer, with its inhibition leading to the suppression of lung cancer cell proliferation and invasion, as well as the inhibition of lung cancer initiation and metastasis [24–26]. Conversely, miR-29c-3p typically exhibits cancer-suppressive characteristics and is downregulated in various cancer tissues [27–31]. A study has reported that miR-29c-3p may negatively regulate the biological behavior of lung cancer cells [32]. In this study, the upregulation of exosomal miR-1290 and downregulation of miR-29c-3p were demonstrated in both all lung cancer patients and early-stage lung cancer patients. Hence, it is plausible that exosomal miR-1290 and miR-29c-3p play a role in the initiation and progression of lung cancer, and the dysregulation of their expression levels may aid in early detection.

Additionally, we assessed the diagnostic effectiveness of exosomal miR-1290 and miR-29c-3p for lung cancer. To ensure practicality and convenience in clinical diagnosis, we established the optimal cutoff value to distinguish between lung cancer or early-stage lung cancer and benign lung diseases in the testing group, and converted exosomal miRNA levels into binary data in the validation group. Exosomal miR-1290 and miR-29c-3p exhibited superior discriminatory potential in distinguishing between lung cancer and benign lung diseases compared to conventional serum tumor markers. Particularly, in the case of early-stage lung cancer, exosomal miR-1290 and miR-29c-3p demonstrated enhanced diagnostic efficacy in comparison to commonly used serum tumor markers. Although the widespread adoption of LDCT screening has facilitated the identification of a greater number of pulmonary nodules, the more effective and accurate identification of malignant nodules, as well as the optimization of pulmonary nodule management, necessitates further endeavors [33]. This study provided evidence that exosomal miR 1290 and miR-29c-3p possessed significant diagnostic efficacy in early-stage lung cancer detection. Moreover, these exosomal miRNAs could be utilized to explore abnormalities

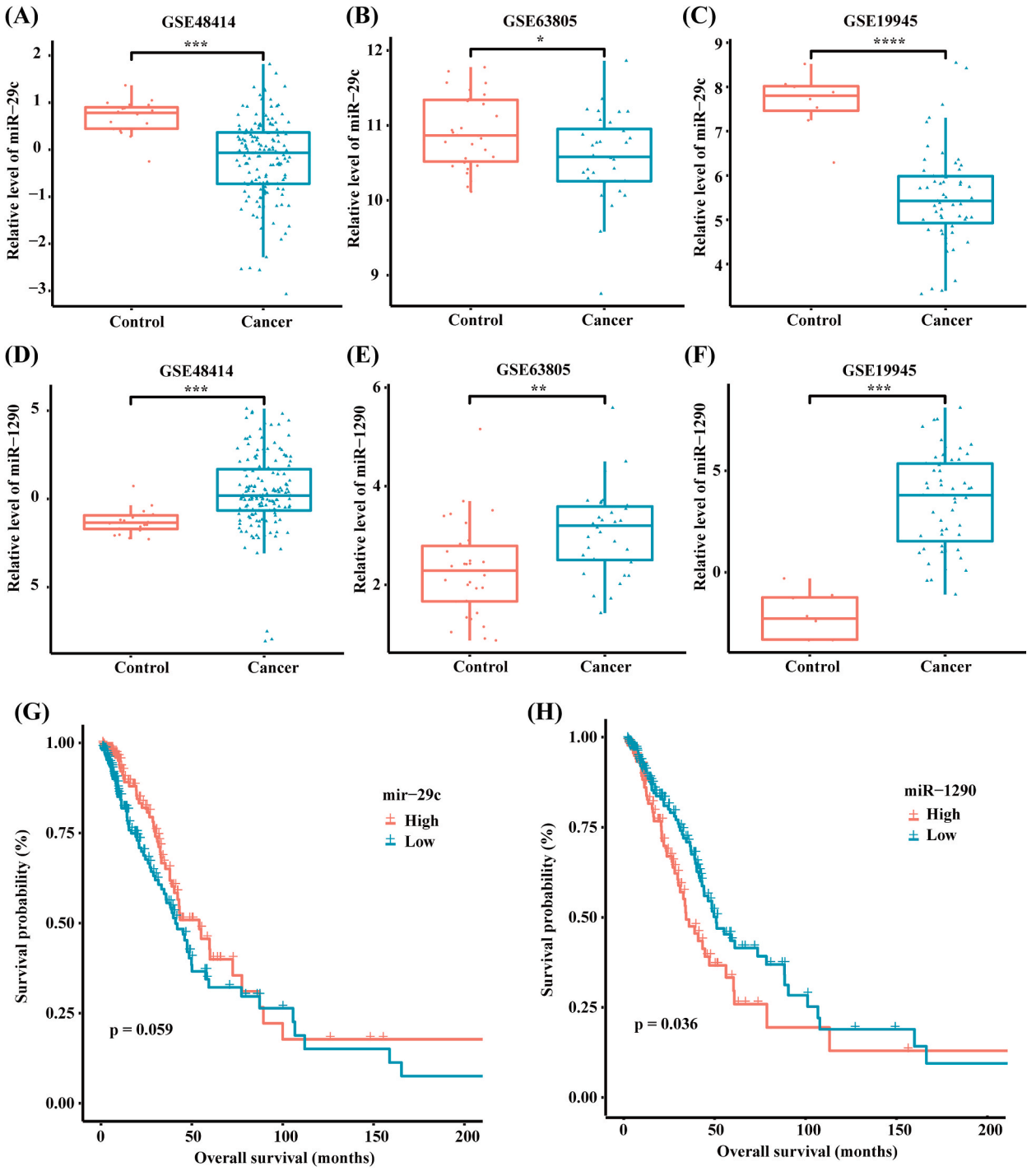

Fig. 7. Differential expression of miRNAs between lung cancer tissues and normal lung tissues. The expression level of miR-29c in GSE48414 **(A)**, GSE63805 **(B)**, and GSE19945 **(C)**. The expression level of miR-1290 in GSE48414 **(D)**, GSE63805 **(E)**, and GSE19945 **(F)**. The prognostic evaluation of miR-29c **(G)** and miR-1290 **(H)** in lung adenocarcinoma based on TCGA database. TCGA, The Cancer Genome Atlas; ***, $P < 0.001$; **, $P < 0.01$.

identified by LDCT, thereby mitigating the rates of false-positive results and overdiagnosis associated with LDCT. Additionally, their implementation could enhance the management of pulmonary nodules.

Furthermore, both exosomal miR-1290 and miR-29c-3p exhibited substantial discriminatory potential between NSCLC and SCLC, with their combination yielding superior diagnostic efficiency compared to that of the individual miRNAs. The accurate classification of histological subtypes is crucial for determining effective treatments for lung cancer. In cases where biopsy specimens cannot be

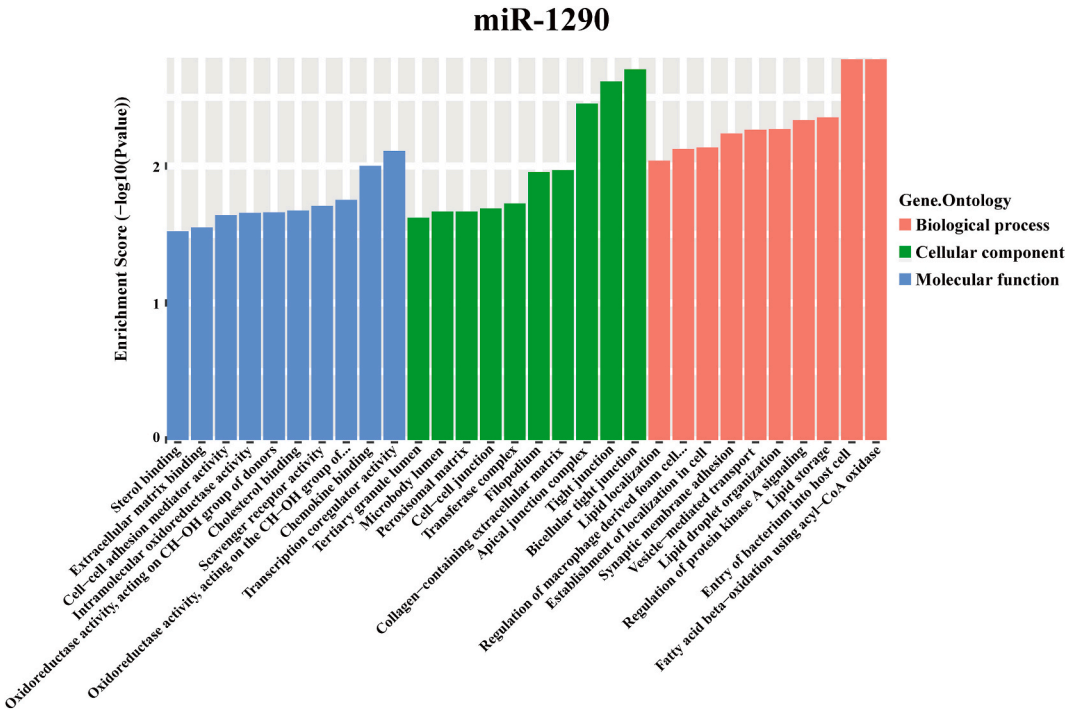

Fig. 8. The molecular function, cellular component, and biological process of potential target genes of miR-1290 based on GO enrichment analysis. TOP 10 items of each functional category are shown in the bar plot. GO, Gene ontology.

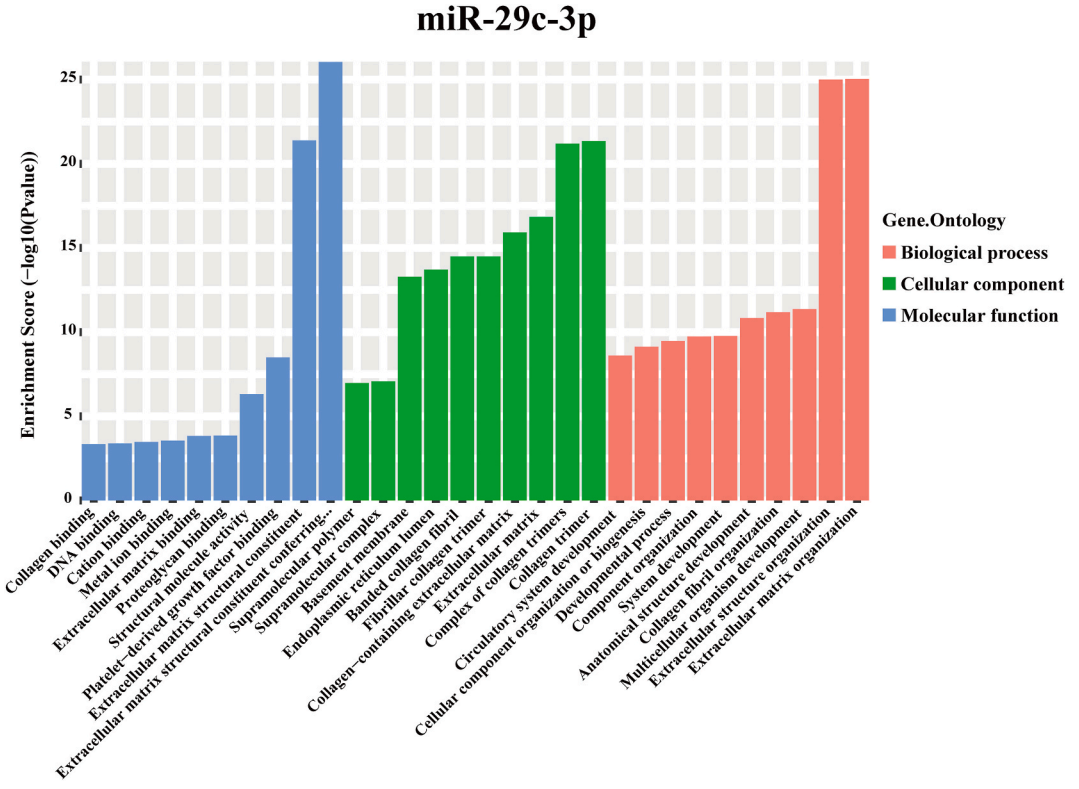

Fig. 9. The molecular function, cellular component, and biological process of potential target genes of miR-29c-3p based on GO enrichment analysis. TOP 10 items of each functional category are shown in the bar plot. GO, Gene ontology.

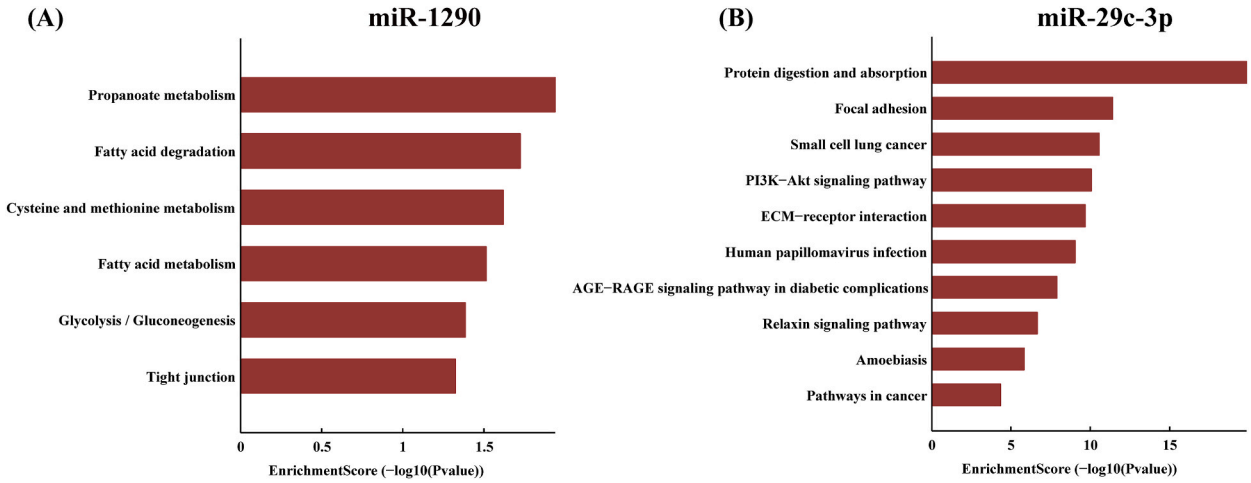

Fig. 10. The biological pathways involved in potential target genes of miR-1290 **(A)** and miR-29c-3p **(B)** based on KEGG pathway analysis. KEGG, Kyoto Encyclopedia of Genes and Genomes.

obtained, cytopathological examination is essential for the diagnosis of lung cancer. However, relying solely on cytology for the accurate diagnosis of histological subtypes is challenging due to uncertain tissue structure, inadequate cell differentiation, or a limited number of tumor cells [34]. As a result, exosomal miR-1290 and miR-29c-3p had the potential to serve as noninvasive biomarkers for diagnosing lung cancer subtypes and guiding treatment.

The findings of our study indicated a significant association between the overexpression of exosomal miR-1290 and advanced clinical stage, advanced T stage, and metastasis in lung cancer. This aligns with a previous investigation that demonstrated a positive correlation between elevated miR-1290 expression in lung cancer tissue and advanced tumor stage and lymph node metastasis [25]. These results suggested that exosomal miR-1290 might serve as a crucial communication mediator between lung cancer cells and the tumor microenvironment, thereby playing a pivotal role in the progression of lung cancer. Consequently, the substantial upregulation of exosomal miR-1290 could potentially serve as a reliable indicator of lung cancer progression. However, no significant associations were observed between the expression of exosomal miR-29c-3p and various clinicopathological features, including clinical stage, T stage, lymph node metastasis, or distant metastasis. This lack of correlation may be attributed to the role of miR-29c-3p as a downregulated tumor suppressor miRNA, primarily involved in the initiation of lung cancer. Once lung cancer cells acquire enhanced proliferation and invasion capabilities, the expression of exosomal miR-29c-3p appears to stabilize throughout the progression of the disease.

Additionally, our findings indicated a significant correlation between elevated levels of miR-1290 in lung adenocarcinoma tissue and decreased overall survival, while decreased expression of miR-29c suggested an unfavorable prognosis. This observation was further supported by Yu's study, which demonstrated that low miR-29c expression was linked to poor outcomes in lung cancer [35]. Furthermore, several investigations have reported a relationship between miR-1290 expression in both serum and NSCLC tissues and the responsiveness of NSCLC patients to anti-tumor therapies [24,36]. Moreover, the expression level of miR-29c-3p in NSCLC tissues has been associated with the risk of NSCLC recurrence in patients undergoing cisplatin chemotherapy after resection [37]. Hence, it is imperative to further investigate and validate the potential of exosomal miR-1290 and miR-29c-3p as biomarkers for monitoring treatment response and prognosis evaluation.

5. Conclusions

The findings of this study elucidated the significant diagnostic efficacy of exosomal miR-1290 and miR-29c-3p in distinguishing lung cancer patients, particularly those in the early stages, from individuals with benign lung disease. Moreover, both exosomal miR-1290 and miR-29c-3p demonstrated remarkable discriminatory capabilities between NSCLC and SCLC. These will effectively enhance the management of pulmonary nodules and facilitate the discrimination of lung cancer subtypes. Hence, the findings of this study indicated that exosomal miR-1290 and miR-29c-3p hold significant potential as biomarkers for the early detection of lung cancer and discrimination between NSCLC and SCLC.

Ethics approval and consent to participate

This study was approved by the Medical Ethics Committee of Tangdu Hospital (K202011-14) and written informed consent was obtained from each participant. All procedures conform to the provisions of the Declaration of Helsinki.

Availability of data and materials

The dataset(s) supporting the conclusions of this article are available in the [Gene Expression Omnibus] repository, [GSE196159, https://www.ncbi.nlm.nih.gov/geo/query/acc.cgi].

Funding

This work was supported by the National Natural Science Foundation of China (Grant No. 81970076), Achievements Cultivation Program of Tangdu Hospital (Grant No. 2020CGPY001) and Military Clinical New High-tech Program (Grant No. 2010gxjs081).

CRediT authorship contribution statement

Qian Zhang: Writing – original draft, Writing – review & editing. **Kaifu Zheng:** Methodology, Writing – review & editing. **Yongheng Gao:** Methodology. **Shihong Zhao:** Methodology. **Yabo Zhao:** Software. **Wangping Li:** Validation. **Yandong Nan:** Data curation. **Zhengping Li:** Data curation. **Wei Liu:** Software. **Xinxin Wang:** Visualization. **Yanwei Chen:** Conceptualization. **Gang Liu:** Supervision. **Faguang Jin:** Project administration, Resources, Supervision.

Declaration of competing interest

The authors declare that they have no known competing financial interests or personal relationships that could have appeared to influence the work reported in this paper.

Acknowledgements

Not applicable.

Appendix A. Supplementary data

Supplementary data to this article can be found online at https://doi.org/10.1016/j.heliyon.2023.e21059.

References

[1] H. Sung, J. Ferlay, R.L. Siegel, et al., Global cancer statistics 2020: GLOBOCAN Estimates of incidence and mortality worldwide for 36 cancers in 185 countries, CA Cancer J Clin 71 (3) (2021) 209–249, https://doi.org/10.3322/caac.21660.
[2] A.A. Thai, B.J. Solomon, L.V. Sequist, J.F. Gainor, R.S. Heist, Lung cancer, Lancet 398 (10299) (2021) 535–554, https://doi.org/10.1016/s0140-6736(21)00312-3.
[3] K.D. Miller, L. Nogueira, A.B. Mariotto, et al., Cancer treatment and survivorship statistics, 2019. CA Cancer J Clin 69 (5) (2019) 363–385, https://doi.org/10.3322/caac.21565.
[4] D.R. Aberle, A.M. Adams, C.D. Berg, et al., Reduced lung-cancer mortality with low-dose computed tomographic screening, N. Engl. J. Med. 365 (5) (2011) 395–409, https://doi.org/10.1056/NEJMoa1102873.
[5] P.M. Boiselle, Computed tomography screening for lung cancer, JAMA 309 (11) (2013) 1163–1170, https://doi.org/10.1001/jama.2012.216988.
[6] W. Chang, J. Zhu, D. Yang, et al., Plasma versican and plasma exosomal versican as potential diagnostic markers for non-small cell lung cancer, Respir. Res. 24 (1) (2023 May 31) 140, https://doi.org/10.1186/s12931-023-02423-4.
[7] J.W.P. Bracht, C. Mayo-de-Las-Casas, J. Berenguer, et al., The present and future of liquid biopsies in non-small cell lung cancer: combining four biosources for diagnosis, prognosis, prediction, and disease monitoring, Curr. Oncol. Rep. 20 (9) (2018 Jul 20) 70, https://doi.org/10.1007/s11912-018-0720-z.
[8] C. Bailey, J.R.M. Black, J.L. Reading, et al., Tracking cancer Evolution through the disease course, Cancer Discov. 11 (4) (2021 Apr) 916–932, https://doi.org/10.1158/2159-8290.CD-20-1559.
[9] E. Kilgour, D.G. Rothwell, G. Brady, et al., Liquid biopsy-based biomarkers of treatment response and resistance, Cancer Cell 37 (4) (2020 Apr 13) 485–495, https://doi.org/10.1016/j.ccell.2020.03.012.
[10] C. Masaoutis, C. Mihailidou, G. Tsourouflis, S. Theocharis, Exosomes in lung cancer diagnosis and treatment. From the translating research into future clinical practice, Biochimie 151 (2018) 27–36, https://doi.org/10.1016/j.biochi.2018.05.014.
[11] E. Smolle, V. Taucher, J. Lindenmann, M. Pichler, F.M. Smolle-Juettner, Liquid biopsy in non-small cell lung cancer-current status and future outlook-a narrative review, Transl. Lung Cancer Res. 10 (5) (2021) 2237–2251, https://doi.org/10.21037/tlcr-21-3.
[12] L. Cheng, R.A. Sharples, B.J. Scicluna, A.F. Hill, Exosomes provide a protective and enriched source of miRNA for biomarker profiling compared to intracellular and cell-free blood, J. Extracell. Vesicles 3 (2014), https://doi.org/10.3402/jev.v3.23743.
[13] C. Hu, S. Meiners, C. Lukas, G.T. Stathopoulos, J. Chen, Role of exosomal microRNAs in lung cancer biology and clinical applications, Cell Prolif. 53 (6) (2020), e12828, https://doi.org/10.1111/cpr.12828.
[14] B. Langmead, C. Trapnell, M. Pop, S.L. Salzberg, Ultrafast and memory-efficient alignment of short DNA sequences to the human genome, Genome biology 10 (3) (2009) R25, https://doi.org/10.1186/gb-2009-10-3-r25.
[15] M.D. Robinson, D.J. McCarthy, G.K. Smyth, edgeR: a Bioconductor package for differential expression analysis of digital gene expression data, Bioinformatics 26 (1) (2010) 139–140, https://doi.org/10.1093/bioinformatics/btp616.
[16] D.J. McCarthy, Y. Chen, G.K. Smyth, Differential expression analysis of multifactor RNA-Seq experiments with respect to biological variation, Nucleic acids research 40 (10) (2012) 4288–4297, 17.1093/nar/gks042.
[17] K.J. Livak, T.D. Schmittgen, Analysis of relative gene expression data using real-time quantitative PCR and the 2(-Delta Delta C(T)) Method, Methods (San Diego, Calif) 25 (4) (2001) 402–408, https://doi.org/10.1006/meth.2001.1262.
[18] Y.L. Wu, Q. Zhou, Clinical trials and biomarker research on lung cancer in China, Expert Opin. Ther. Targets 16 (Suppl 1) (2012) S45–S50, https://doi.org/10.1517/14728222.2011.630663.

[19] M. Salehi, M. Sharifi, Exosomal miRNAs as novel cancer biomarkers: challenges and opportunities, J. Cell. Physiol. 233 (9) (2018) 6370–6380, https://doi.org/10.1002/jcp.26481.
[20] M. Kobayashi, K. Sawada, K. Nakamura, et al., Exosomal miR-1290 is a potential biomarker of high-grade serous ovarian carcinoma and can discriminate patients from those with malignancies of other histological types, J. Ovarian Res. 11 (1) (2018) 81, https://doi.org/10.1186/s13048-018-0458-0.
[21] Y. Shi, Y. Zhuang, J. Zhang, M. Chen, S. Wu, Four circulating exosomal miRNAs as novel potential biomarkers for the early diagnosis of human colorectal cancer, Tissue Cell 70 (2021), 101499, https://doi.org/10.1016/j.tice.2021.101499.
[22] Q. Wang, G. Wang, L. Niu, et al., Exosomal MiR-1290 promotes angiogenesis of hepatocellular carcinoma via targeting SMEK1, Journal of oncology 2021 (2021), 6617700, https://doi.org/10.1155/2021/6617700.
[23] J. Huang, M. Shen, M. Yan, et al., Exosome-mediated transfer of miR-1290 promotes cell proliferation and invasion in gastric cancer via NKD1, Acta biochimica et biophysica Sinica 51 (9) (2019) 900–907, https://doi.org/10.1093/abbs/gmz077.
[24] W.C. Zhang, T.M. Chin, H. Yang, et al., Tumour-initiating cell-specific miR-1246 and miR-1290 expression converge to promote non-small cell lung cancer progression, Nat. Commun. 7 (2016), 11702, https://doi.org/10.1038/ncomms11702.
[25] J.J. Jin, Y.H. Liu, J.M. Si, R. Ni, J. Wang, Overexpression of miR-1290 contributes to cell proliferation and invasion of non small cell lung cancer by targeting interferon regulatory factor 2, Int. J. Biochem. Cell Biol. 95 (2018) 113–120, https://doi.org/10.1016/j.biocel.2017.12.017.
[26] L. Wu, T. Liu, Y. Xiao, et al., Polygonatum odoratum lectin induces apoptosis and autophagy by regulation of microRNA-1290 and microRNA-15a-3p in human lung adenocarcinoma A549 cells, Int. J. Biol. Macromol. 85 (2016) 217–226, https://doi.org/10.1016/j.ijbiomac.2015.11.014.
[27] H. Xu, H.L. Mao, X.R. Zhao, Y. Li, P.S. Liu, MiR-29c-3p, a target miRNA of LINC01296, accelerates tumor malignancy: therapeutic potential of a LINC01296/miR-29c-3p axis in ovarian cancer, J. Ovarian Res. 13 (1) (2020) 31, https://doi.org/10.1186/s13048-020-00631-w.
[28] C. Chen, Z. Huang, X. Mo, et al., The circular RNA 001971/miR-29c-3p axis modulates colorectal cancer growth, metastasis, and angiogenesis through VEGFA, Journal of experimental & clinical cancer research : CR 39 (1) (2020) 91, https://doi.org/10.1186/s13046-020-01594-y.
[29] K. Lu, F. Feng, Y. Yang, et al., High-throughput screening identified miR-7-2-3p and miR-29c-3p as metastasis suppressors in gallbladder carcinoma, J. Gastroenterol. 55 (1) (2020) 51–66, https://doi.org/10.1007/s00535-019-01627-0.
[30] M. Dobre, V. Herlea, C. Vlăduţ, et al., Dysregulation of miRNAs targeting the IGF-1R pathway in pancreatic ductal adenocarcinoma, Cells 10 (8) (2021), https://doi.org/10.3390/cells10081856.
[31] J. Chen, W. Lou, B. Ding, X. Wang, Overexpressed pseudogenes, DUXAP8 and DUXAP9, promote growth of renal cell carcinoma and serve as unfavorable prognostic biomarkers, Aging 11 (15) (2019) 5666–5688, https://doi.org/10.18632/aging.102152.
[32] Y. Li, Y. Liu, K. Jin, et al., Negatively regulated by miR-29c-3p, MTFR1 promotes the progression and glycolysis in lung adenocarcinoma via the AMPK/mTOR signalling pathway, Front. Cell Dev. Biol. 9 (2021), 771824, https://doi.org/10.3389/fcell.2021.771824.
[33] K. Xi, W. Wang, Y. Wen, et al., Combining plasma miRNAs and computed tomography features to differentiate the nature of pulmonary nodules, Front. Oncol. 9 (2019) 975, https://doi.org/10.3389/fonc.2019.00975.
[34] W. Huang, J. Hu, D.W. Yang, et al., Two microRNA panels to discriminate three subtypes of lung carcinoma in bronchial brushing specimens, Am. J. Respir. Crit. Care Med. 186 (11) (2012) 1160–1167, https://doi.org/10.1164/rccm.201203-0534OC.
[35] D.H. Yu, X.L. Ruan, J.Y. Huang, et al., Analysis of the interaction network of hub miRNAs-hub genes, being involved in idiopathic pulmonary fibers and its Emerging role in non-small cell lung cancer, Front. Genet. 11 (2020) 302, https://doi.org/10.3389/fgene.2020.00302.
[36] M. Saito, K. Shiraishi, K. Matsumoto, et al., A three-microRNA signature predicts responses to platinum-based doublet chemotherapy in patients with lung adenocarcinoma, Clin. Cancer Res. 20 (18) (2014) 4784–4793, https://doi.org/10.1158/1078-0432.Ccr-14-1096.
[37] D.M. Sun, B.F. Tang, Z.X. Li, et al., MiR-29c reduces the cisplatin resistance of non-small cell lung cancer cells by negatively regulating the PI3K/Akt pathway, Sci. Rep. 8 (1) (2018) 8007, https://doi.org/10.1038/s41598-018-26381-w.